Supplementary Information

Over 31% Efficient Indoor Organic Photovoltaics Enabled by Simultaneously Reduced Trap-assisted Recombination and Non-radiative Recombination Voltage Loss

Xiaobo Zhou,[a] *Hongbo Wu*,[b] *Urvashi Bothra*,[c] *Xingze Chen*,[d] *Guanyu Lu*,[e] *Heng Zhao*,[a] *Chao Zhao*,[a] *Qun Luo*,[d] *Guanghao Lu*,[e] *Ke Zhou*,*[a] *Dinesh Kabra*,*[c] *Zaifei Ma**[b] and *Wei Ma**[a]

[a]X. Zhou, H. Zhao, B. Lin, Dr. C. Zhao, Dr. K. Zhou, Prof. W. Ma

State Key Laboratory for Mechanical Behavior of Materials, Xi'an Jiaotong University, Xi'an 710049, China

[b]H. Wu, Z. Ma

Advanced Low-dimension Materials, State Key Laboratory for Modification of Chemical Fibers and Polymer Materials, Center for College of Materials Science and Engineering, Donghua University, Shanghai 201620, China.

[c]U. Bothra, D. Kabra

Department of Physics, Indian Institute of Technology, Mumbai, 400076 India.

[d]X. Chen, Q. Luo

Frontier Institute of Science and Technology, Xi'an Jiaotong University, Xi'an 710054, China.

[e]G. Lu, G. Lu

i-Lab & Printable Electronics Research Center, Suzhou Institute of Nano-Tech and Nano-Bionics, Chinese Academy of Sciences, Suzhou, 215123 China.

*Corresponding author. E-mail: dkabra@phy.iitb.ac.in; mazaifei@dhu.edu.cn; msekzhou@xjtu.edu.cn; msewma@xjtu.edu.cn

Experiment section

Materials. PM6 was purchased from Solarmer Materials Inc. Y6-O was purchased from eFlesPV Limited.

Fabrication and measurements of OPVs.

The organic solar cells were fabricated with a conventional structure of ITO/PEDOT:PSS/PM6:Y6-O/PDINO/Al. The patterned ITO substrates were cleaned by sonication in detergent water, deionized water, acetone and isopropanol for 20 min of each step. After the UVO treatment for 20 min, an hole-transporting layer of PEDOT:PSS was deposited by spin-coating at 5500 rpm for 30 s, followed by thermal annealing at 140 °C for 10 min. The BHJ active layer solution was prepared in chloroform (with 20 mg/ml DBCL) at a total concentration of 20 mg/mL with the D/A ratio of 1:1 by weight. For the LBL device, the PM6 and Y6-O were prepared in chloroform at a concentration of 9 mg/mL (with 9 mg/ml DBCL) and 12 mg/mL (with 20 mg/ml DBCL). The solution was stirred on a hotplate at 50 °C at least 6 h. We firstly deposited PM6 layer, then the Y6-O was seqeuntially deposited in the glovebox. Both the thickness of BHJ and LBL active layer is 110 nm. The film thickness of LBL film is carefully tuned by change the spin-coating speed of PM6 and Y6-O. Then the films are transferred to vacuum for 30 min, followed by thermal annealing at 80 °C for 10 min. PDINO methanol solution (2.0 mg/mL) was then spin-coated on the active layer at 3300 rpm for 30 s to afford a buffer layer with

a thickness of 10 nm. Finally, 100 nm Al was sequentially deposited as top electrode under vacuum (<1×10^{-4} Pa). The *J-V* characteristics were performed in N2-filled glovebox under AM 1.5G (100 mW/cm^2) by using a Keithley 2400 source meter unit and an AAA solar simulator (SS-F5-3A, Enli Technology CO., Ltd.) calibrated by a standard Si photovoltaic cell with a KG5 filter. The EQE was measured by a solar cell spectral response measurement system (QE-R3018, Enli Technology CO., Ltd.) with the calibrated light intensity by a standard single-crystal Si photovoltaic cell. The spectra irradiation of the LED was measured by using a calibrated high-precision fibre-optics spectrometer (Maya2000 Pro, Ocean Optics). The UV–Vis absorption spectra were measured on a Shimadzu UV-3600 Plus Spectrophotometer. Photoluminescence (PL) spectra were performed on PTI Quanta Master™ 400 UV/VIS Spectrofluorometer at the excitation wavelength of 780 nm.

EL, EQE_{EL}, sensitive-EQE (SEQE), and TPV measurements.

Electroluminescence measurement utilized the direct-current meter (PWS2326, Tectronix) to offer bias voltage to the device, then the luminous signals were collected by fluorescence spectrometer (KYMERA-328I-B2,Andor technology LTD). The EQE-EL measurement system basically includes Keithley 2400 digital source meter, Keithley 6482 picoammeters and a standard Si detector (S1337-1010Br). For the sensitive-EQE measurement, the light from halogen light source (LSH-75, Newport) became monochromatic light by using a monochromator (CS260-RG-3-MC-A, Newport), and was focused on the device to generate electrical signals. Then the signals were amplified by the front-end current amplifier (SR570, Stanford) and finally collected by the phase-locked amplifier (Newport).

The EQE spectrum can be obtained by using the corrected Si standard detector (S1337-1010Br). For TPV mensurement, the background illumination was provided by a normal LED light source, and pulsed light was provided by arbitrary wave generator (AFG322C, Tektronix), eventually, the transient photovoltage signals for the device was collected by oscilloscope (MDO4104C, Tektronix).

Grazing Incidence Wide-Angle X-ray Scattering (GIWAXS) Characterization. GIWAXS measurements were performed at beamline 7.3.3 at the Advanced Light Source. Samples were prepared on Si substrates using identical blend solutions as those used in devices. The 10 keV X-ray beam was incident at a grazing angle of 0.11°-0.15°, selected to maximize the scattering intensity from the samples. The scattered x-rays were detected using a Dectris Pilatus 2M photon counting detector.

Resonant Soft X-ray Scattering (RSoXS). RSoXS transmission measurements were performed at beamline 11.0.1.2 at the Advanced Light Source (ALS). Samples for R-SoXS measurements were prepared on a PSS modified Si substrate under the same conditions as those used for device fabrication, and then transferred by floating in water to a 1.5 mm × 1.5 mm, 100 nm thick Si_3N_4 membrane supported by a 5 mm × 5 mm, 200 μm thick Si frame (Norcada Inc.). 2-D scattering patterns were collected on an in-vacuum CCD camera (Princeton Instrument PI-MTE). The sample detector distance was calibrated from diffraction peaks of a triblock copolymer poly(isoprene-b-styrene-b-2-vinyl pyridine), which has a known spacing of 391 Å. The beam size at the sample is approximately 100 μm by 200 μm.

AFM measurements. The surface topography of the active layer was recorded by atomic force microscopy (AFM) operated in the tapping mode.

Hole and electron mobility measurements. The mobilities were measured by using space charge limited current (SCLC) model with the hole-only device of ITO/PEDOT:PSS/PM6:Y6-O/MoO3/Al and electron-only device of ITO/ZnO/PM6:Y6-O/PDINO/Al. Hole mobility and electron mobility were obtained by fitting the current density-voltage curves and calculated by the equation:

$$J = 9\varepsilon_0\varepsilon_r\mu(V_{appl} - V_{bi} - V_s)^2/8L^3$$

Where J is current density, ε_0 is the permittivity of free space, ε_r is the relative permittivity of the material (assumed to 3), μ is hole mobility or electron mobility, V_{appl} is applied voltage, V_{bi} is the built-in voltage (0 V), V_s is the voltage drop from the substrate's series resistance (V_s =IR) and L is the thickness of film.

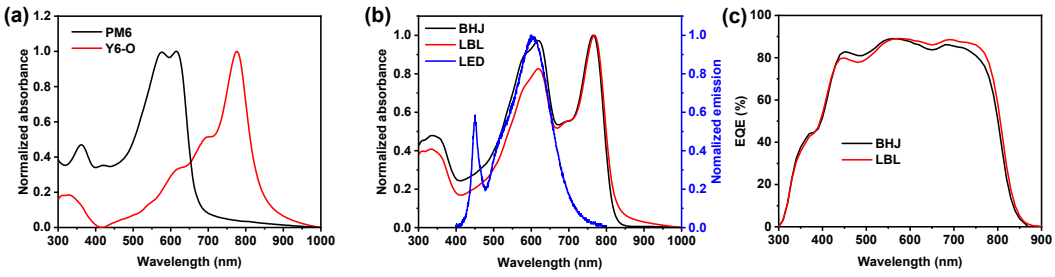

Figure S1. (a) UV-vis absorption spectra of PM6 and Y6-O films; (b) UV-vis absorption spectra of PM6:Y6-O based BHJ and LBL films and emission spectra of LED; (c) EQE curves of BHJ and LBL devices.

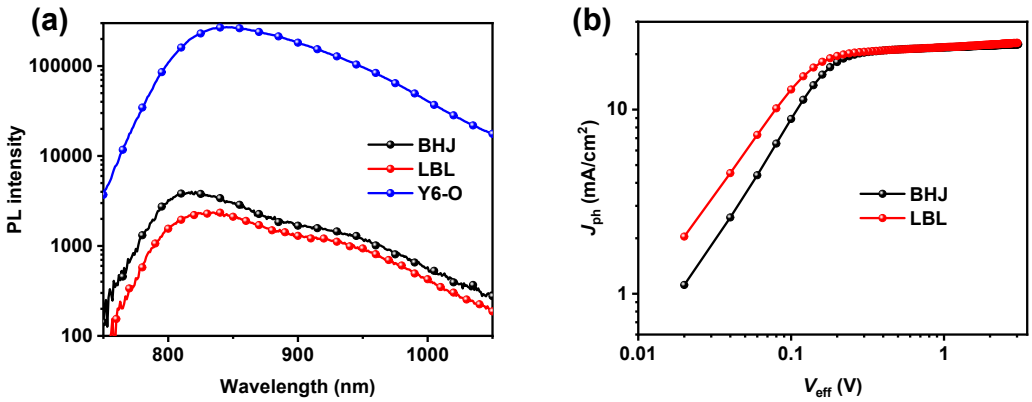

Figure S2. (a) Photoluminescence spectra of Y6-O neat film, PM6:Y6-O based BHJ and LBL films; (b) J_{ph}–V_{eff} curves of BHJ and LBL devices under 1 sun intensity.

Table S1. The PL quenching rate of corresponding films and calculated P_{diss} from J_{ph}-V_{eff} curves.

Active layer	PL quenching rate (%)	P_{diss} (%)
BHJ	98.2	95.7
LBL	99.0	96.8

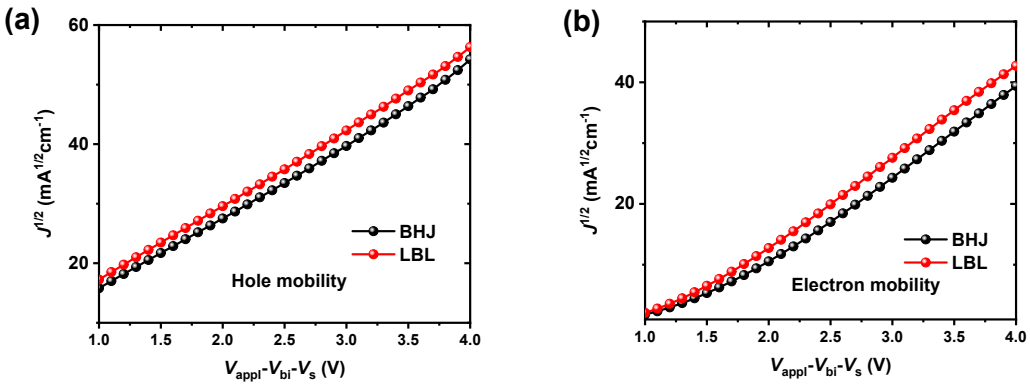

Figure S3. $J^{1/2}$ -V characteristics of (a) hole-only and (b) electron-only devices based on BHJ and LBL films.

Table S2. The calculated hole-mobility, electron mobility and their ratios from $J^{1/2}$ -V curves.

Condition	μ_h ($\times10^{-4}$ $cm^2V^{-1}S^{-1}$)[a]	μ_e ($\times10^{-4}$ $cm^2V^{-1}S^{-1}$)[a]	μ_h/μ_e
BHJ	1.23 (1.17±0.07)	1.07 (1.05±0.05)	1.15
LBL	1.27 (1.22±0.06)	1.24 (1.20±0.05)	1.02

[a] The average parameters were calculated from more than 10 independent cells.

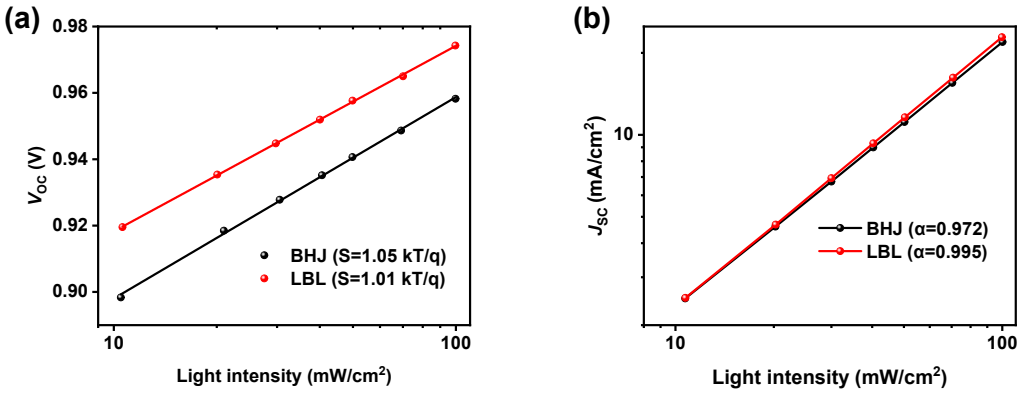

Figure S4. Dependence of (a) V_{OC} and (b) J_{SC} on light intensity of BHJ and LBL devices.

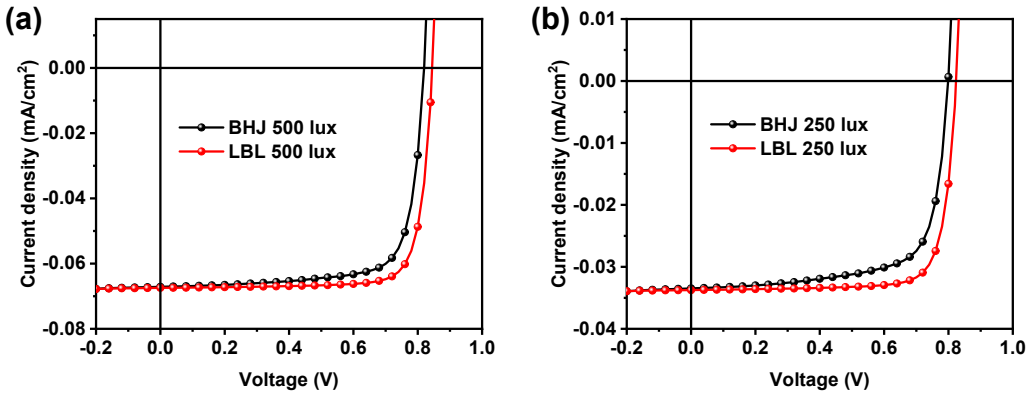

Figure S5. *J-V* curves of BHJ and LBL devices under (a) 500 lux and (b) 250 lux LED illuminance.

Table S3. The corresponding photovoltaic parameters of indoor devices reported in the literature.

Active layer	Illumination (lux)	V_{OC} (V)	J_{SC} (μA/cm^2)	FF (%)	PCE (%)	Ref.
OD:$PC_{71}BM$:PDI2	1000	0.64	127.1	70	20.5	[1]
PM6:IT-4F	1000	0.712	113	78.0	20.8	[2]
OD:PC71BM:IDT	1000	0.63	132.9	71.7	29.9	[1]
CD1:PBN-14	1000	1.06	116	62.6	24.9	[3]
CD1:PBD-10	1000	1.14	105	65.4	21.7	[4]
PM6:ITCC	1000	0.962	95.8	72.0	22.0	[2]
PM6:Y-TH2:Y6	1000	0.701	320	74.48	22.33	[5]
PBTZT-sat-BDTT-8:$PC_{61}BM$:$PC_{71}BM$	1000	0.81	112.4	70.4	23.1	[6]
PBDB-TF:IO-4Cl	1000	1.10	90.6	79.1	26.1	[7]
PB2:F-BTA3	1000	1.08	98.1	78.8	27.1	[8]
PBQx-TCl:BTA3:BTP-eC9	1000	1.10	97.7	80.1	28.5	[9]
PM6:FCC-Cl	2000	0.914	244.1	81.2	28.5	[10]
J51-Cl:BTA3:BTA1	1000	1.118	96.65	80.27	28.84	[11]
Copolymer:PCBM	1000	0.650	143	71	29	[12]
PBDB-T:GS-ISO	1000	1.09	98.2	80.36	29.15	[13]
D18:FCC-Cl	2000	0.975	245.4	80.1	30.1	[10]
PM6:ITIC-Th:IT-4F	500	0.75	74.73	77.10	30.11	[14]
PB2:FTCC-Br	1000	0.943	123.8	81.1	30.2	[15]

PM6:Y6-O	1650	0.84	245	76.0	31.01	[16]
PM6:Y6-O (BHJ)	1000	0.840	133.8	78.4	28.8	This work
PM6:Y6-O (LBL)	1000	0.866	134.9	81.5	31.2	This work

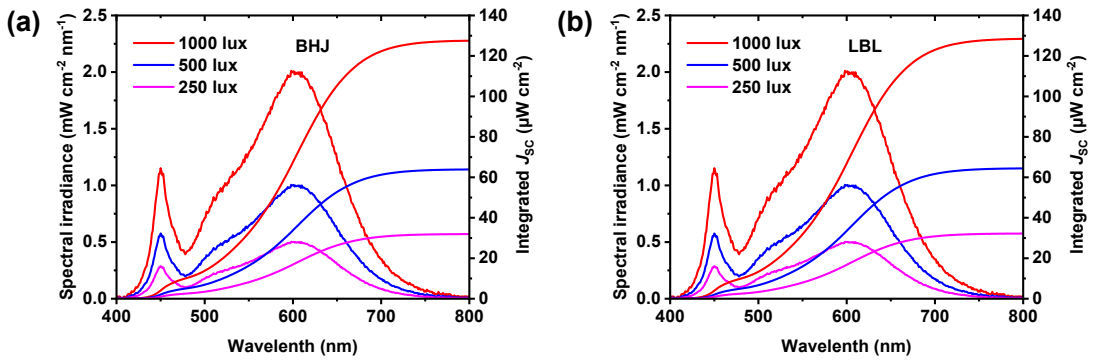

Figure S6. The LED at 1000, 500 and 250 lux and corresponding integrated current density of the (a) BHJ and (b) LBL devices.

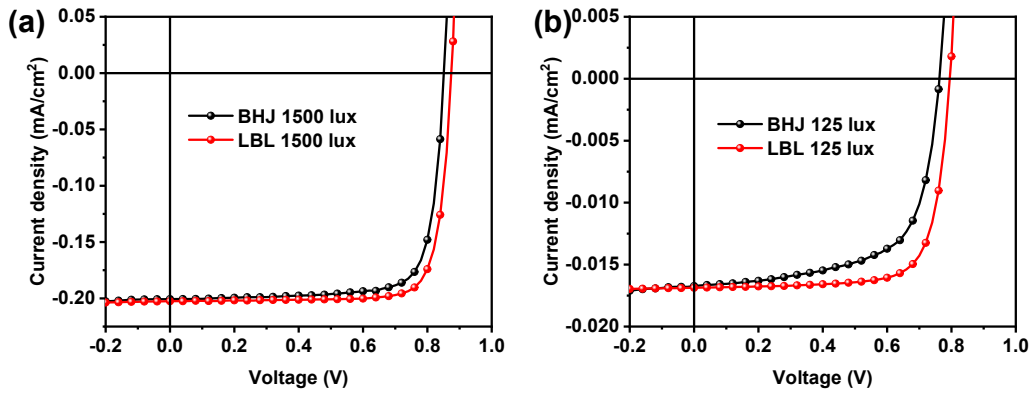

Figure S7. *J-V* curves of BHJ and LBL devices under (a) 1500 lux; (b) 125 lux LED illuminance.

Table S4. The photovoltiac parameters of BHJ and LBL devices under 1500 and 125 lux LED.

Active layer	Light intensity (lux)	V_{OC} (V)	J_{SC} (μA·cm^{-2})	FF (%)	PCE (%)[a]
BHJ	1500	0.851	200.7	79.1	29.3 (28.7±0.7)
	125	0.762	16.7	65.3	21.8 (20.7±0.8)
LBL	1500	0.875	202.5	81.4	31.5 (30.6±0.7)
	125	0.795	16.8	75.8	26.6 (25.8±0.6)

[a] The average parameters were calculated from more than 10 independent cells.

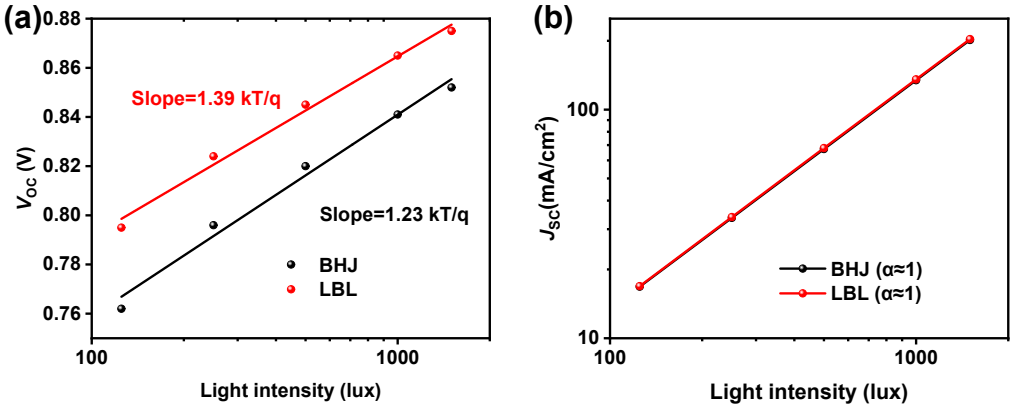

Figure S8. Dependence of (a) V_{OC} and (b) J_{SC} on indoor light intensity of BHJ and LBL devices.

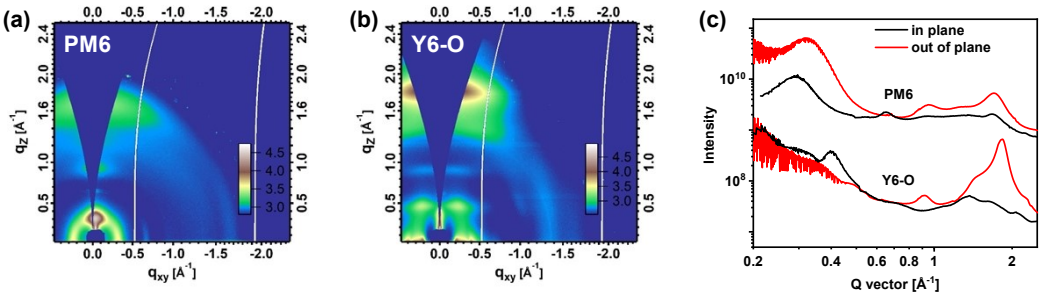

Figure S9. GIWAXS 2D profiles of (a) PM6 and (b) Y6-O films; (c) GIWAXS line profiles of corresponding films.

Table S5. Structure parameters of corresponding films obtained from GIWAXS and RSoXS.

Active layer	Peak location ($Å^{-1}$)	CL (Å)	Domain size (nm)	Domain purity
BHJ	1.80	27.3	20.7	0.97
LBL	1.80	27.8	22.5	1

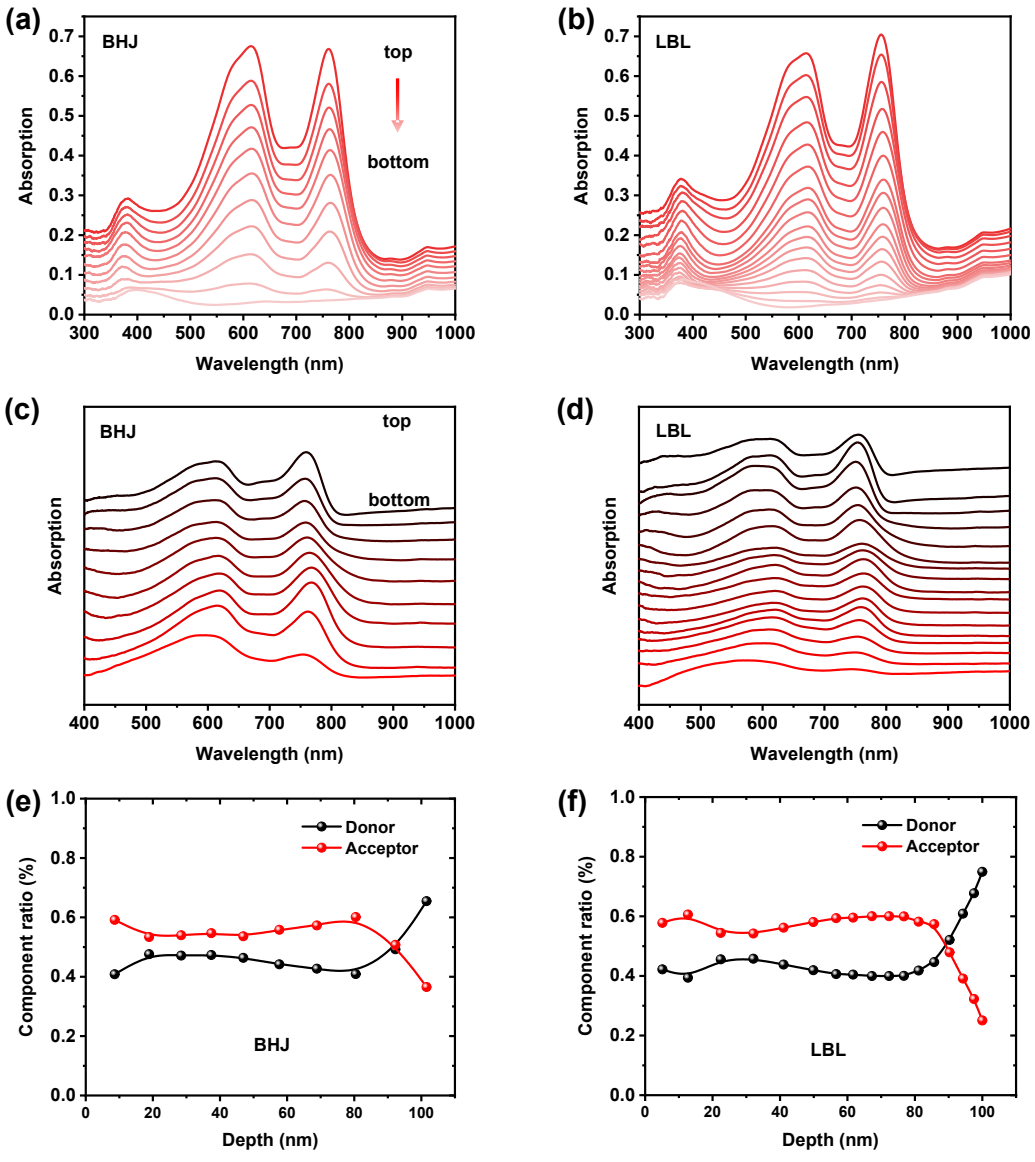

Figure S10. Film-depth-dependent absorption spectra of (a) BHJ and (b) LBL films; and the deduced sub-layer absorption spectra of (c) BHJ and (d) LBL films. Each sub-layer of BHJ and LBL film is about 10 nm and 6 nm; the calculated component ratio of (e) BHL and (f) LBL films.

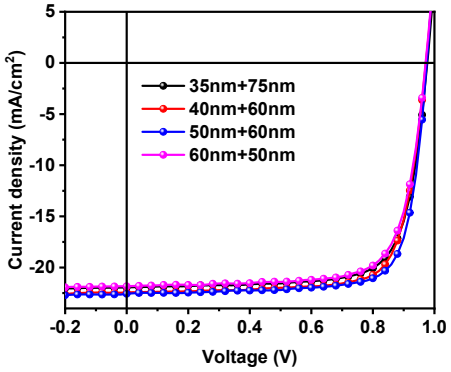

Figure S11. The *J-V* curves of LBL devices with different PM6 and Y6-O thickness under 1 sun light intensity.

Table S6. Photovoltaic parameters of the LBL devices with various PM6 and Y6-O thickness under 1 sun illumination.

PM6/Y6-O Thickness	V_{OC} (V)	J_{SC} (μA cm^{-2})	FF (%)	PCE (%)[a]
35nm+75nm	0.977	21.9	74.8	16.2 (15.5±0.6)
40nm+70nm	0.972	22.4	76.4	16.8 (16.3±0.3)
50nm+60nm	0.975	22.8	77.5	17.2 (16.8±0.5)
60nm+50nm	0.971	21.8	74.7	15.9 (15.2±0.5)

[a] The average parameters were calculated from more than 10 independent cells.

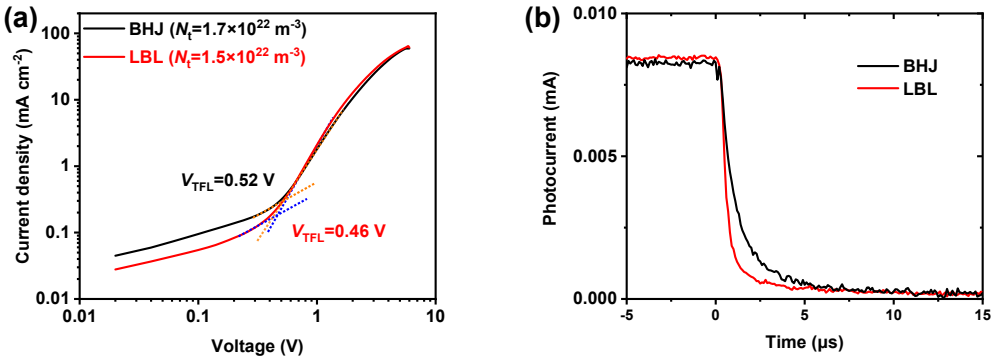

Figure S12. (a) The *J*-*V* curves of electron-only device; (b) Non-normalized photocurrent transient of BHJ and LBL devices.

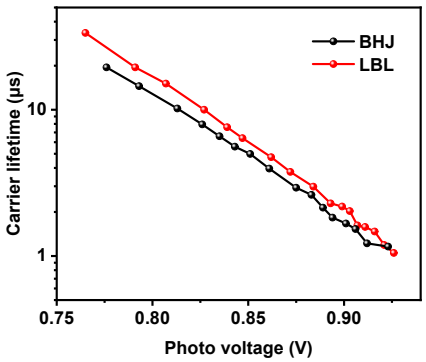

Figure S13. Carrier lifetime of BHJ and LBL devices obtained from TPV measurements.

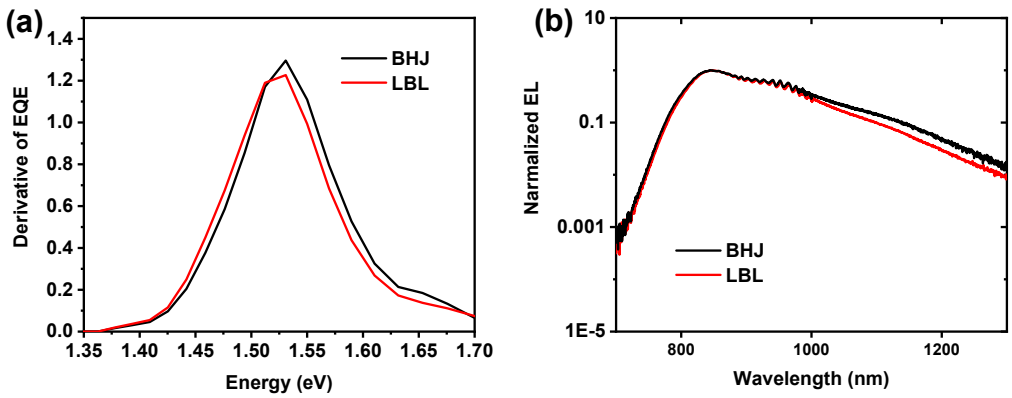

Figure S14. (a) The derivative of the EQE; (b) EL spectra for the BHJ and LBL devices.

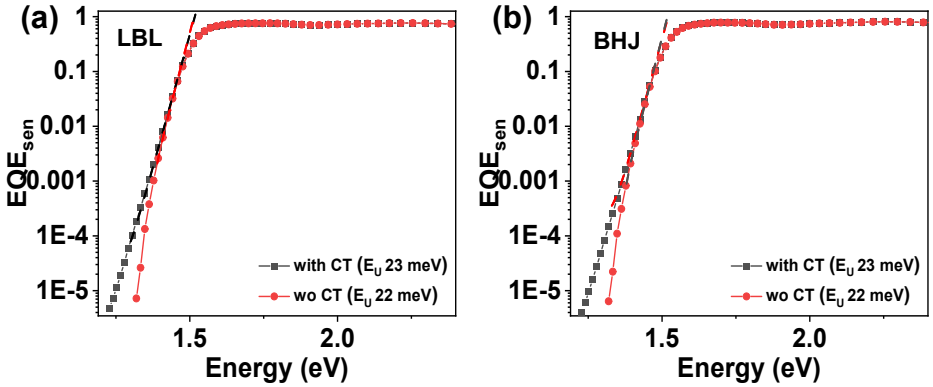

Figure S15. High-sensitive EQE of (a) LBL and (b) BHJ devices with and w/o the CT state absorption.

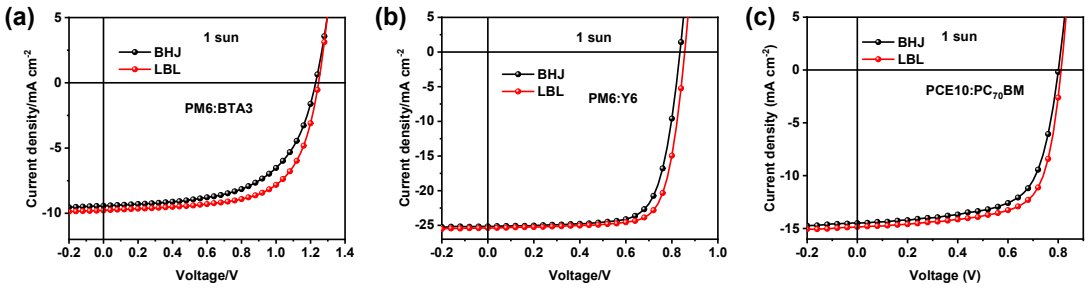

Figure S16. The *J-V* curves of (a) PM6:BTA3; (b) PM6:Y6 and (c) PCE10:$PC_{70}BM$ devices under 1 sun.

Table S7. Photovoltaic parameters of the PM6:BTA3, PM6:Y6 and PCE10:$PC_{70}BM$ devices under 1 sun illumination.

Active layer	Condition	V_{OC} (V)	J_{SC} (mA·cm^{-2})	FF (%)	PCE (%)[a]	R_{sh}/Ω·cm^2
PM6:BTA3	BHJ	1.230	9.42	58.3	6.77 (6.52±0.3)	6.25×10^4
PM6:BTA3	LBL	1.232	9.56	61.5	7.26 (7.03±0.2)	1.10×10^6
PM6:Y6	BHJ	0.841	25.1	74.9	15.8 (15.5±0.2)	4.13×10^4
PM6:Y6	LBL	0.842	25.4	76.0	16.3 (16.0±0.4)	1.78×10^5
PCE10:$PC_{70}BM$	BHJ	0.801	14.5	66.6	7.73 (7.42±0.5)	6.03×10^4
PCE10:$PC_{70}BM$	LBL	0.809	14.9	69.3	8.36 (8.12±0.3)	1.31×10^5

[a] The average parameters were calculated from more than 10 independent cells.

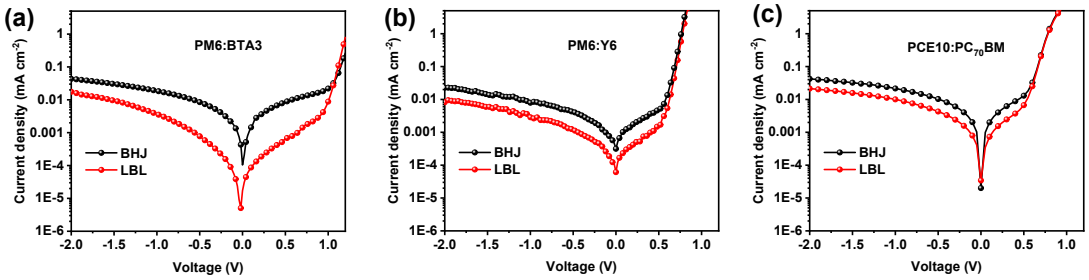

Figure S17. The dark current curves of (a) PM6:BTA3; (b) PM6:Y6 and (c) PCE10:$PC_{70}BM$ devices.

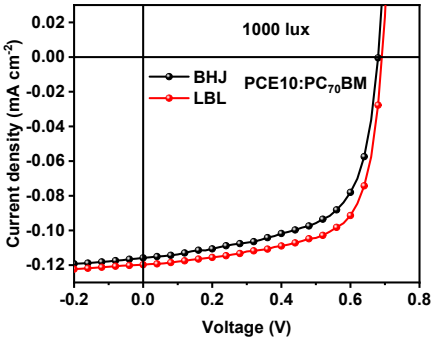

Figure S18. The *J-V* curves of BHJ and LBL devices based on PCE10:$PC_{70}BM$ systems under 1000 lux LED.

Table S8. Photovoltaic parameters of the PM6:BTA3, PM6:Y6 and PCE10:$PC_{70}BM$ devices under 1000 lux LED.

Active layer	Condition	V_{OC} (V)	J_{SC} (μA·cm^{-2})	FF (%)	PCE (%)[a]
PM6:BTA3	BHJ	1.064	81.5	66.4	18.9 (18.2±0.6)
PM6:BTA3	LBL	1.088	83.8	71.5	21.4 (21.0±0.5)
PM6:Y6	BHJ	0.682	133.1	68.6	20.3 (19.7±0.8)
PM6:Y6	LBL	0.701	136.0	73.4	22.9 (22.5±0.6)
PCE10:$PC_{70}BM$	BHJ	0.678	115.2	62.8	16.0 (15.3±0.8)
PCE10:$PC_{70}BM$	LBL	0.691	120.1	67.2	18.1 (17.8±0.5)

[a] The average parameters were calculated from more than 10 independent cells.

References

[1] R. Singh, T. Duan, Z. Kan, C. L. Chochos, G. P. Kini, M. Kumar, J. Park, J. Lee, J.-J. Lee, *Nano Energy*, 2020, **75**, 104934.

[2] Y. Cui, H. Yao, T. Zhang, L. Hong, B. Gao, K. Xian, J. Qin, J. Hou, *Adv. Mater.*, 2019, **31**, 1904512.

[3] J. Wang, Y. Gao, Y. Yu, R. Zhao, L. Zhang, J. Liu, *Organic Electronics*, 2021, **92**, 106134.

[4] Z. C. Ding, R. Y. Zhao, Y. J. Yu, J. Liu, *J. Mater. Chem. A*, 2019, **7**, 26533.

[5] Y. Cho, T. Kumari, S. Jeong, S. M. Lee, M. Jeong, B. Lee, J. Oh, Y. Zhang, B. Huang, L. Chen, C. Yang, *Nano Energy*, 2020, **75**, 104896.

[6] Y. J. You, C. E. Song, Q. V. Hoang, Y. Kang, J. S. Goo, D. H. Ko, J. J. Lee, W. S. Shin, J. W. Shim, *Adv. Funct. Mater.*, 2019, **29**, 1901171.

[7] Y. Cui, Y. M. Wang, J. Bergqvist, H. F. Yao, Y. Xu, B. W. Gao, C. Y. Yang, S. Q. Zhang, O. Inganas, F. Gao, J. H. Hou, *Nat. Energy*, 2019, **4**, 768.

[8] T. Zhang, C. An, Y. Cui, J. Zhang, P. Bi, C. Yang, S. Zhang, J. Hou, *Adv. Mater.*, 2022, **34**, e2105803.

[9] Y. Xu, Y. Cui, H. Yao, T. Zhang, J. Zhang, L. Ma, J. Wang, Z. Wei, J. Hou, *Adv. Mater.*, 2021, **33**, 2101090.

[10] F. Bai, J. Zhang, A. Zeng, H. Zhao, K. Duan, H. Yu, K. Cheng, G. Chai, Y. Chen, J. Liang, W. Ma, H. Yan, *Joule*, 2021, **5**, 1231.

[11] Q. Wu, Y. Yu, X. Xia, Y. Gao, T. Wang, R. Sun, J. Guo, S. Wang, G. Xie, X. Lu, E. Zhou, J. Min, *Joule*, 2022, 10.1016/j.joule.2022.07.001.

[12] B. H. S. Miranda, L. d. Q. Corrêa, G. A. Soares, J. L. Martins, P. L. Lopes, M. L. Vilela, J. F. Rodrigues, T. G. Cunha, R. d. Q. Vilaça, S. Castro-Hermosa, L. Wouk, D. Bagnis, *Sol. Energy*, 2021, **220**, 343.

[13] P. Bi, S. Zhang, J. Ren, Z. Chen, Z. Zheng, Y. Cui, J. Wang, S. Wang, T. Zhang, J. Li, Y. Xu, J. Qin, C. An, W. Ma, X. Hao, J. Hou, *Adv. Mater.*, 2022, **34**, e2108090.

[14] C. Lee, J. H. Lee, H. H. Lee, M. Nam, D. H. Ko, *Adv. Energy Mater.*, 2022, **12**, 2200275.

[15] T. Zhang, C. An, Y. Xu, P. Bi, Z. Chen, J. Wang, N. Yang, Y. Yang, B. Xu, H. Yao, X. Hao, S. Zhang, J. Hou, *Adv. Mater.*, 2022, e2207009.

[16] L.-K. Ma, Y. Chen, P. C. Y. Chow, G. Zhang, J. Huang, C. Ma, J. Zhang, H. Yin, A. M. Hong Cheung, K. S. Wong, S. K. So, H. Yan, *Joule*, 2020, **4**, 1486.